Supporting Information

Fluorine-Induced Highly-Reproducible Resistive Switching Performance: Facile Morphology Control through the Transition between J and H Aggregation

Yang Li, [†,‡] *Zhaojun Liu,* [†] *Hua Li,** [†] *Qingfeng Xu,* [†] *Jinghui He,* [†] *and Jianmei Lu** [†]

[†]College of Chemistry, Chemical Engineering and Materials Science, Soochow University, Suzhou 215123, P. R. China

[‡]School of Materials Science and Engineering, Nanyang Technological University, Singapore 639798, Singapore

Corresponding Author: lihuaw@suda.edu.cn; lujm@suda.edu.cn

***Materials*:** 4-Nitroaniline, sodium nitrate ($NaNO_3$), *N,N*-dimethylaniline, sodium sulfide hydrate ($Na_2S·9H_2O$), phthalic anhydride, 5-fluorophthalic anhydride, 5,6-difluorophthalic anhydride, 4,5,6,7-tetrafluorophthalic anhydride were purchased from commercial sources (TCI and Sigma Aldrich Ltd.). Unless otherwise noted, all other solvents and reagents were of reagent grade and used as received without purification.

***Synthesis of IDAZO, FIDAZO, F_2IDAZO and F_4IDAZO*:** IDAZO, FIDAZO, F_2IDAZO and F_4IDAZO were successfully prepared by consecutive diazotization-coupling, reduction and condensation reactions in good yields, as shown in Figure S1. The intermediate 2 (*N,N*-dimethyl-4-((4-nitrophenyl)diazenyl)aniline) was synthesized following the previously reported procedure.[1,2]

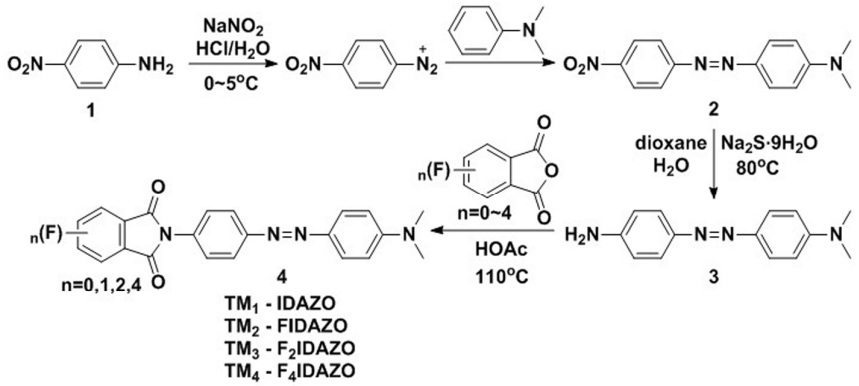

Figure S1. Synthetic routes of target materials IDAZO, FIDAZO, F_2IDAZO and F_4IDAZO.

Synthesis of Intermediates and Final Products

***N,N-dimethyl-4-((4-nitrophenyl)diazenyl)aniline (2)*[1,2]:** 4-Nitroaniline 1 (4.14 g, 30.0 mmol) was added into a mixture of deionized water (12 mL) and concentrated hydrochloric acid (12 mL) under a water bath. Then the mixture was cooled down with an ice bath. After complete cooling, a solution of $NaNO_3$ (2.10g, 30.0 mmol) in deionized water (10 mL) was added dropwise and the mixture gradually became homogeneous. After stirring for 1 h, a cold solution of N,N-dimethylaniline (3.63 g, 30.0 mmol) in a mixture of deionized water (30 mL) and concentrated hydrochloric acid (5 mL) was added slowly for 40 min at 0–5 °C. The mixture was kept stirring for 2 h, and then was neutralized by 1 M KOH aqueous solution to precipitate red powder.

After filtering, the red powder was washed with deionized water and dried over vacuum to obtain the compound 2 with yield of 75%. ^{1}H NMR (400 MHz, $CDCl_3$) δ (ppm): 8.33 (d, J = 8.1 Hz, 2H), 7.93 (d, J = 8.1 Hz, 4H), 6.77 (d, J = 8.2 Hz, 2H), 3.14 (s, 6H).

***N,N-dimethyl-4-((4-aminophenyl)diazenyl)-aniline (3)*:** To a solution of 2 (1.5 g, 5.0 mmol) in dioxane (30 mL), $Na_2S{\cdot}9H_2O$ (2.40 g, 10 mmol) in deionized water (10 mL) was added in portions. Under argon protection, the mixture was heated to 80 ℃ and stirred by monitoring with the thin-layer chromatography (TLC). Once the TLC detected no starting material 2, the reaction mixture was cooled down to room temperature, and then poured into water. After standing for 2 h, the mixture was filtered and fully washed with deionized water. The crude product was dried over vacuum and purified by recrystallization from 50% ethanol to afford 3 as brown solid with yield of 80%. ^{1}H NMR (400 MHz, $CDCl_3$) δ (ppm): 7.78 (dd, J = 32.5, 7.4 Hz, 4H), 6.74 (t, J = 8.4 Hz, 4H), 3.06 (s, 6H).

***2-(4-((4-(dimethylamino)phenyl)diazenyl)phenyl)isoindoline-1,3-dione (IDAZO)*:** Compound 3 (0.48 g, 2 mmol) and phthalic anhydride (0.33g, 2.2 mmol) were dissolved into acetic acid (5 mL) and kept refluxing for 12 h. The reaction mixture was cooled down to room temperature and poured into water. The precipitate was filtered and washed with deionized water for several times. Purification of the crude material through column chromatography on silica gel using a mixed mobile phase of ethyl acetate and petroleum ether yielded the product IDAZO (0.44 g, 60%). ^{1}H NMR (400 MHz, $CDCl_3$) δ (ppm): 8.04–7.75 (m, 8H), 7.59 (d, J = 7.5 Hz, 2H), 6.77 (d, J = 7.9 Hz, 2H), 3.10 (s, 6H). ^{13}C NMR (101 MHz, $CDCl_3$) δ 167.16, 152.56, 152.18, 143.56, 134.47, 132.22, 131.70, 126.79, 125.17, 123.78, 122.76, 111.46, 40.30. HRMS (m/z): calcd for $C_{22}H_{18}N_4O_2$ $[M + H]^+$ 371.1430, found 371.1503.

***2-(4-((4-(dimethylamino)phenyl)diazenyl)phenyl)-5-fluoroisoindoline-1,3-dione (FIDAZO)*:** Reaction Condition was similar with that for compound **IDAZO**, except 5-fluorophthalic anhydride (0.33g, 2.2 mmol) was used. Purification of the crude material on silica gel by ethyl acetate-petroleum ether as eluent yielded the product FIDAZO (0.61 g, 78%). ^{1}H NMR (400 MHz, $CDCl_3$) δ (ppm): 8.24–7.78 (m, 5H),

7.56 (t, J = 34.1 Hz, 4H), 6.78 (s, 2H), 3.11 (s, 6H). ^{13}C NMR (101 MHz, $CDCl_3$) δ 166.11, 165.83, 152.66, 152.37, 143.64, 134.56, 132.03, 127.55, 126.74, 126.29, 126.20, 125.24, 122.84, 121.72, 121.49, 111.51, 40.33. ^{19}F NMR (376 MHz, $CDCl_3$) δ (ppm): -100.92.

***2-(4-((4-(dimethylamino)phenyl)diazenyl)phenyl)-5,6-difluoroisoindoline-1,3-dione (F_2IDAZO)*:** Reaction Condition was similar with that for compound **IDAZO**, except 5,6-difluorophthalic anhydride (0.33g, 2.2 mmol) was used. Purification of the crude material on silica gel by ethyl acetate-petroleum ether as eluent yielded the product F_2IDAZO (0.65 g, 80%). ^{1}H NMR (400 MHz, $CDCl_3$) δ (ppm): 8.13–7.85 (m, 4H), 7.78 (d, J = 6.8 Hz, 2H), 7.55 (d, J = 8.1 Hz, 2H), 6.80 (s, 2H), 3.12 (s, 6H). ^{13}C NMR (101 MHz, $CDCl_3$) δ 165.13, 155.95, 153.35, 152.67, 131.80, 128.60, 126.66, 125.35, 122.87, 113.75, 113.54, 111.62, 40.39. ^{19}F NMR (376 MHz, $CDCl_3$) δ (ppm): -124.62, -124.63.

***2-(4-((4-(dimethylamino)phenyl)diazenyl)phenyl)-4,5,6,7-tetrafluoroisoindoline-1,3-dione (F_4IDAZO)*:** Reaction Condition was similar with that for compound **IDAZO**, except 4,5,6,7-tetrafluorophthalic anhydride (0.33g, 2.2 mmol) was used. Purification of the crude material on silica gel by ethyl acetate-petroleum ether as eluent yielded the product F_4IDAZO (0.48 g, 54%). ^{1}H NMR (400 MHz, $CDCl_3$) δ (ppm): 8.09–7.88 (m, 4H), 7.52 (d, J = 8.4 Hz, 2H), 6.82 (d, J = 8.2 Hz, 2H), 3.13 (s, 6H). ^{19}F NMR (376 MHz, $CDCl_3$) δ (ppm): -134.92, -134.95, -141.37, -141.40. HRMS (m/z): calcd for $C_{22}H_{16}F_2N_4O_2$ $[M + H]^+$ 443.1053, found 443.1126.

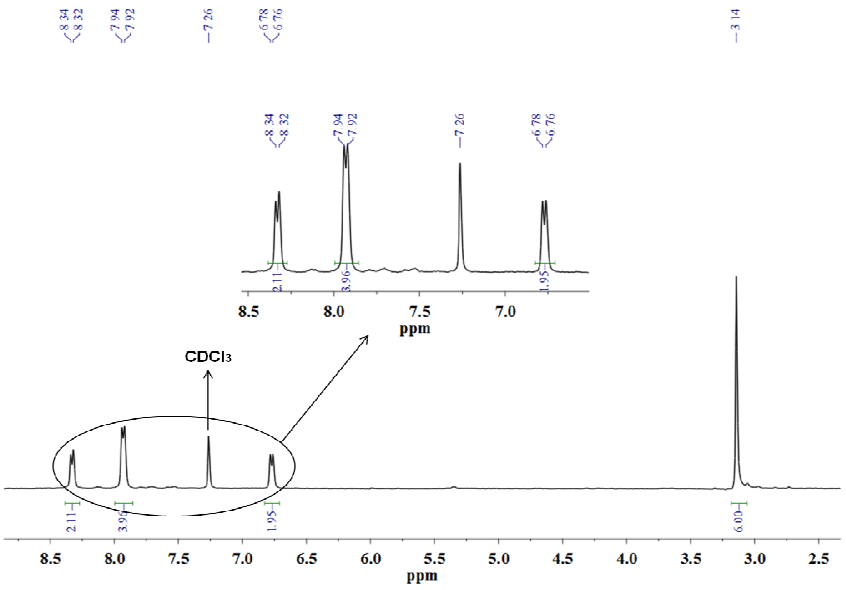

Figure S2. ^{1}H NMR spectrum of intermediate 2 in $CDCl_3$.

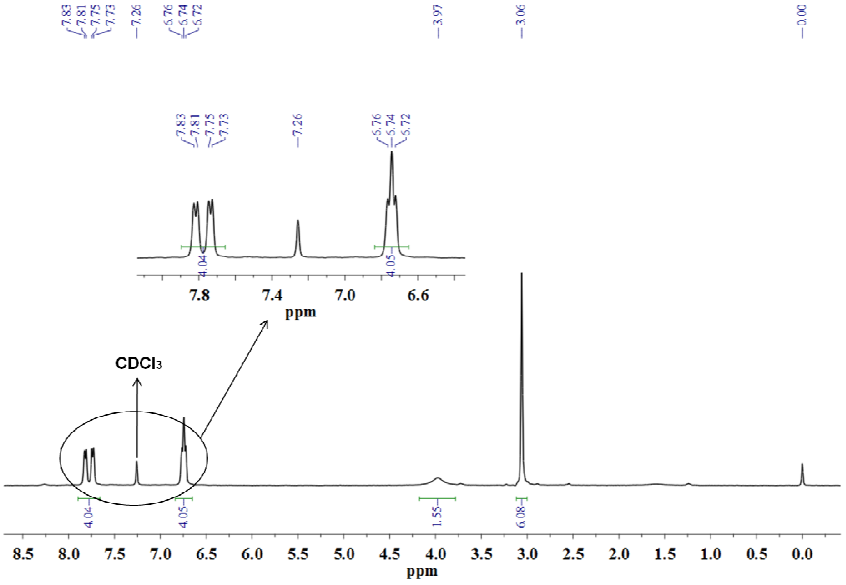

Figure S3. ^{1}H NMR spectrum of intermediate 3 in $CDCl_3$.

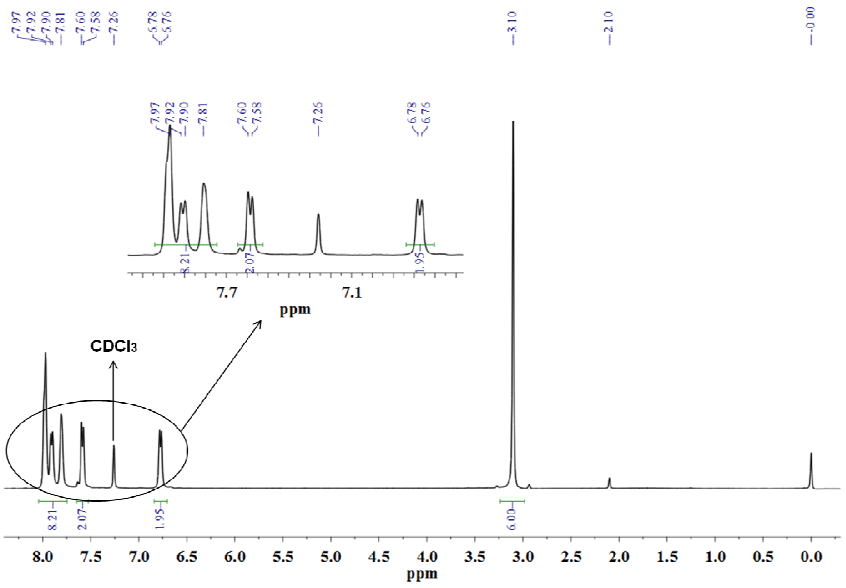

Figure S4. ^{1}H NMR spectrum of IDAZO in $CDCl_3$.

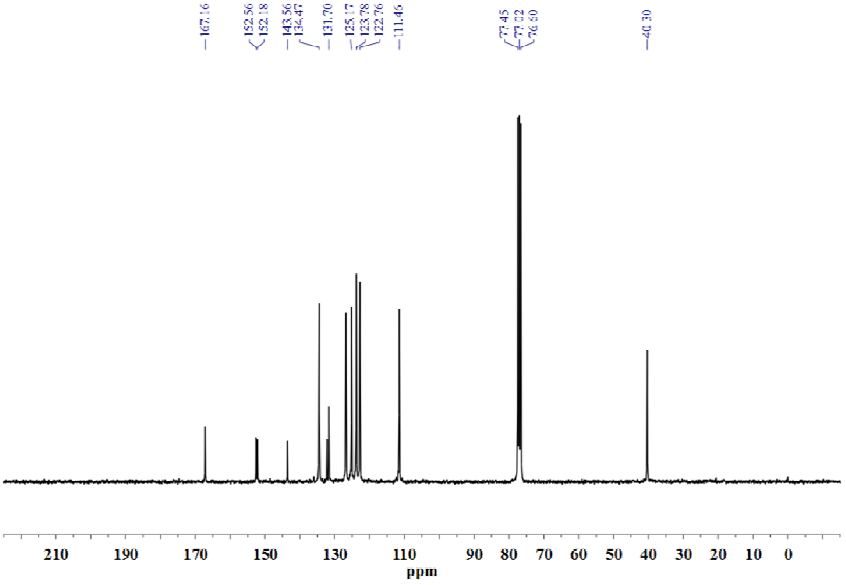

Figure S5. ^{13}C NMR spectrum of IDAZO in $CDCl_3$.

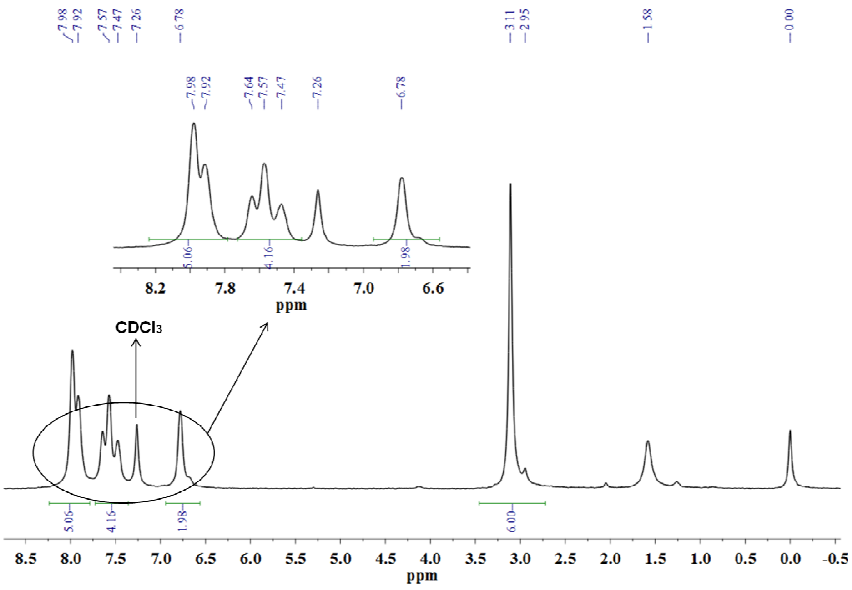

Figure S6. ^{1}H NMR spectrum of FIDAZO in $CDCl_3$.

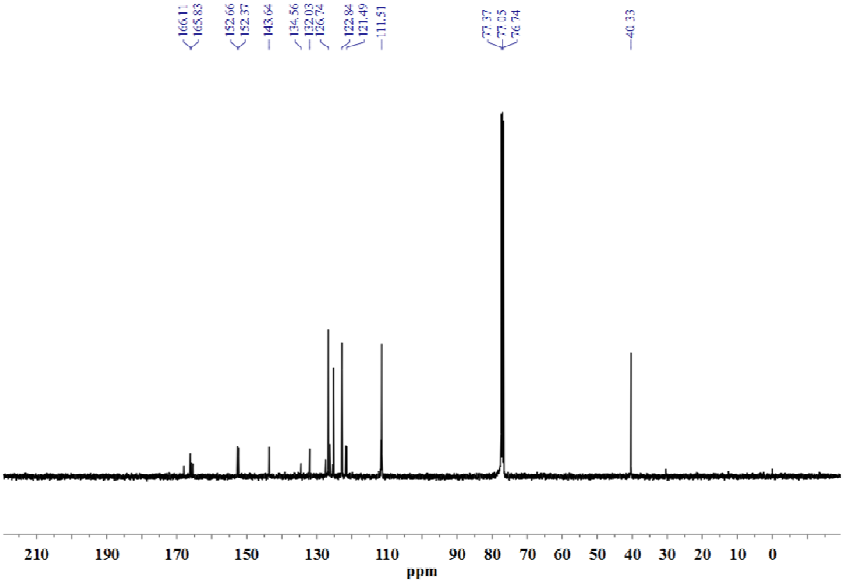

Figure S7. ^{13}C NMR spectrum of FIDAZO in $CDCl_3$.

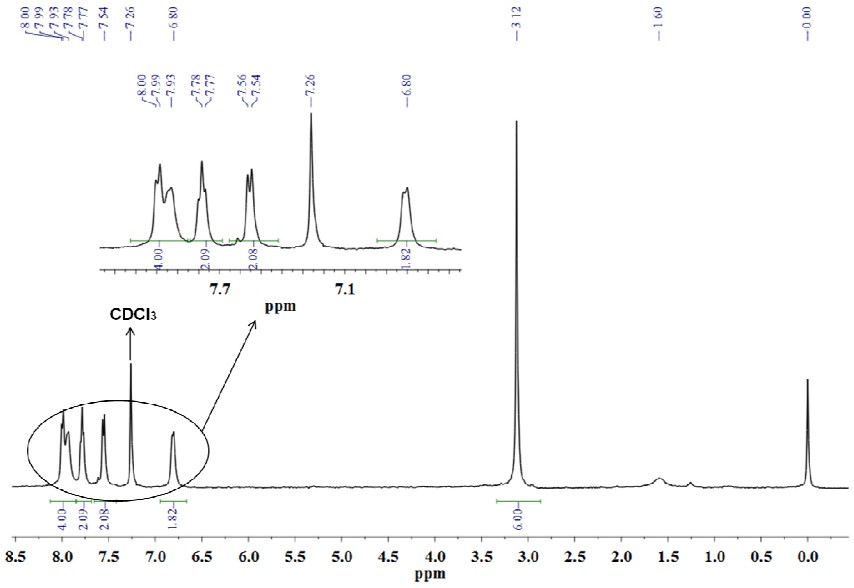

Figure S8. ^{1}H NMR spectrum of F_2IDAZO in $CDCl_3$.

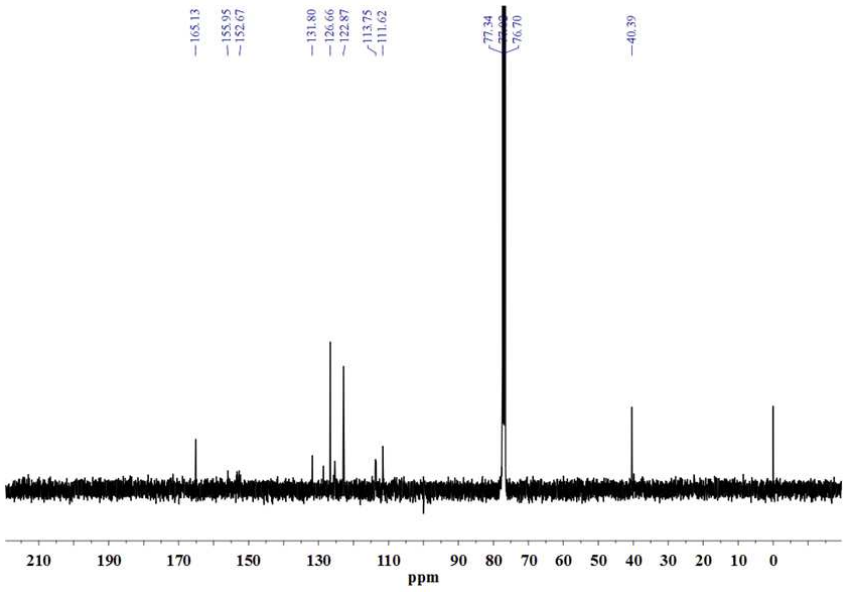

Figure S9. ^{13}C NMR spectrum of F_2IDAZO in $CDCl_3$.

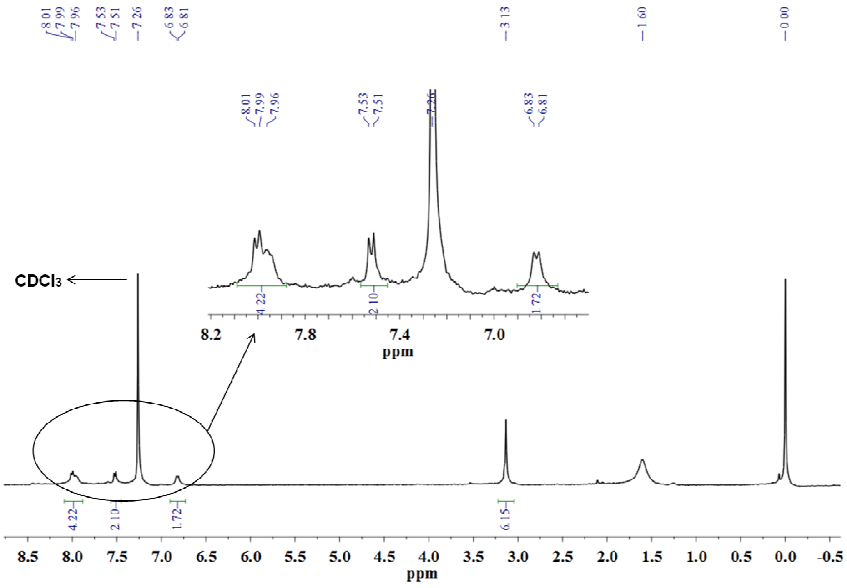

Figure S10. ^{1}H NMR spectrum of F_4IDAZO in $CDCl_3$.

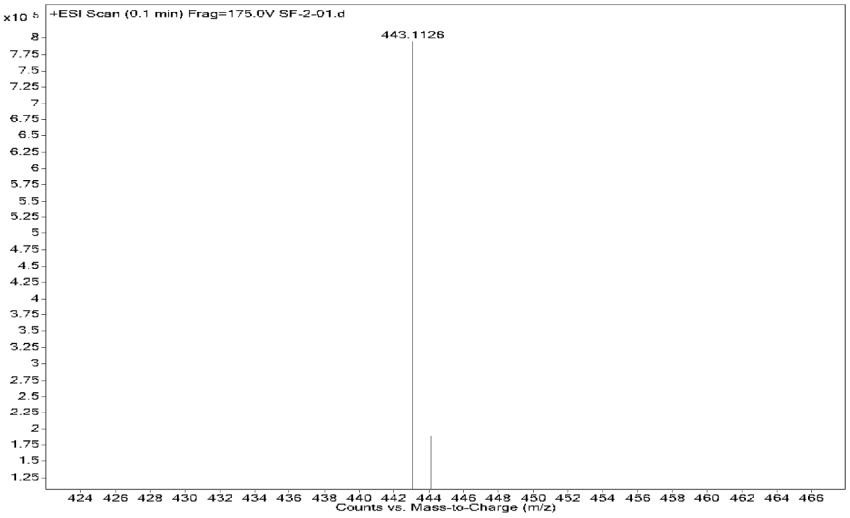

Figure S11. The HR-MS spectrum of F_4IDAZO.

***Measurements and general methods*:** All ^{1}H, ^{13}C and ^{19}F NMR spectra were acquired in chloroform-*d* containing 0.003% TMS as an internal reference with an Inova 400 MHz FT-NMR spectrometer unless otherwise noted. High-resolution mass spectra (HR-MS) were measured on a Micromass GCT-TOF mass spectrometer with ESI resource. Thermo gravimetric analysis (TGA) was conducted at a heating rate of 10 ºC min^{-1} with a TA instrument Dynamic TGA 2950 under a N_2 flow rate of 50 mL min^{-1}. UV–Vis absorption spectra were measured at room temperature with a

Shimadzu UV-3600 spectrophotometer in dichloromethane solvent and on a 2×2 cm^2 quartz cell (film). Fluorescence spectra were obtained by an Edinburgh-920 fluorescence spectra photometer (Edinburgh Co. UK) with a slit of 5 nm. Cyclic voltammograms (CVs) were collected using a three-electrode setup CorrTest CS Electrochemical Workstation analyzer in a solution of 0.1mol/L tetrabutylammonium hexafluorophosphate ($TBAPF_6$) as the supporting electrolyte in anhydrous acetonitrile at a sweep rate of 100 mV/s, with the assistances of an ITO working electrode, a reference electrode Ag/AgCl (KCl saturated), and a counter electrode (Pt wire). For calibration, the external ferrocene/ferrocenium (F_c/F_c^+) redox standard potential was measured under the identical condition (0.34 eV vs.Ag/AgCl), where the absolute redox potential of F_c/F_c^+ is assumed to be −4.80 eV to vacuum. The HOMO and LUMO were calculated according to the following equations: $E_{HOMO} = -[E_{ox}^{onset} + 4.8 - E_{ferrocene}^{1/2}]$ (eV), $E_{LUMO} = E_{HOMO} + E_g$ (eV),[3-5] in which E_{ox}^{onset} is the onset potential for the oxidation process, and E_g is estimated from the optical onset-edge band gap equation: $E_g = 1240/\lambda_{edge}$[3-5]. Scanning electron microscope (SEM) image was performed using a Hitachi S-4700 SEM instrument. Atomic force microscope (AFM) measurements were performed to study the thin film morphology with a MFP-3DTM (Digital Instruments/Asylum Research) AFM instrument in tapping mode. The contact angle (CA) measurements were carried out to characterize the wettability of film surfaces using a DropMeter A-200. X-ray diffraction (XRD) patterns were obtained by an X'Pert-Pro MPD X-ray diffractometer with a Cu KR monochromatic radiation source at 40 kV and 30 mA.

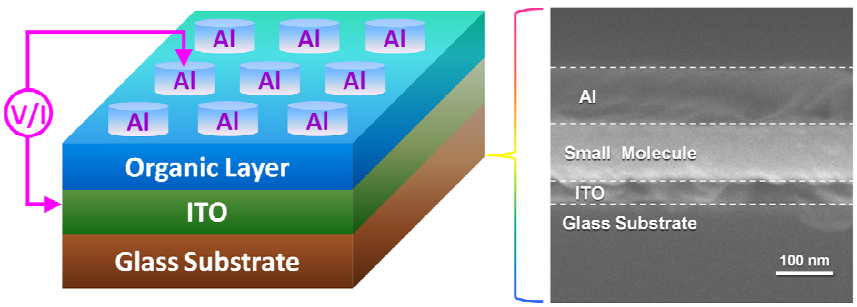

Figure S12. Scheme (left) and Cross-sectional SEM image (right) of the RS device

highlighting the layer-by-layer architecture of organic memory cells.

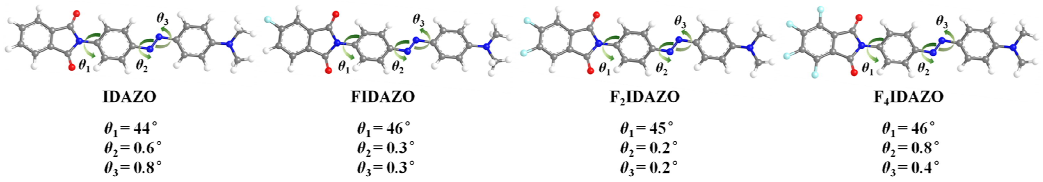

Figure S13. DFT calculated (GGA/BLYP/DNP) optimized geometries of IDAZO, FIDAZO, F_2IDAZO and F_4IDAZO. The four conformations are almost the same.

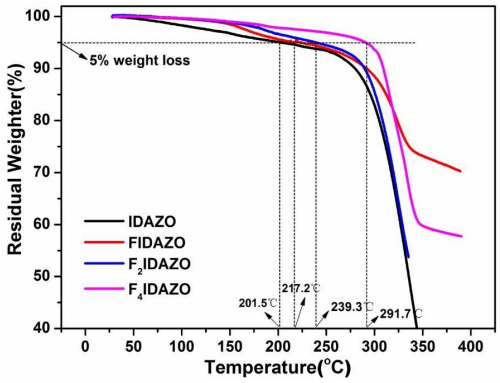

Figure S14. TGA curves of IDAZO, FIDAZO, F_2IDAZO and F_4IDAZO with a heating rate of 10 ºC min^{-1} under a nitrogen atmosphere.

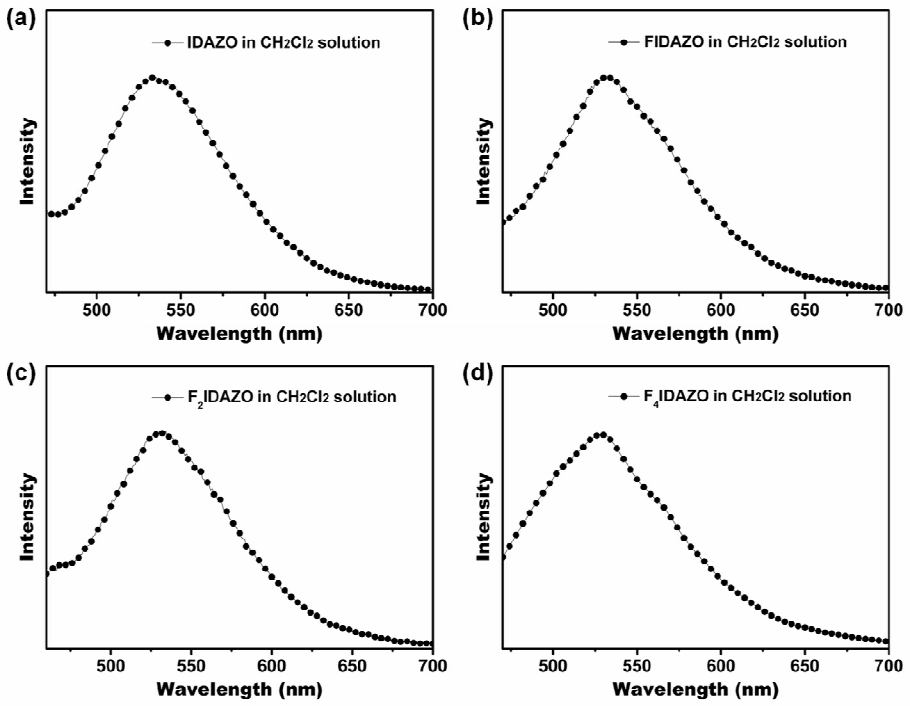

Figure S15. The emission spectra of IDAZO (a), FIDAZO (b), F_2IDAZO (c) and F_4IDAZO (d) in CH_2Cl_2 solution at the same excitation wavelength (λ_{ex} = 460 nm).

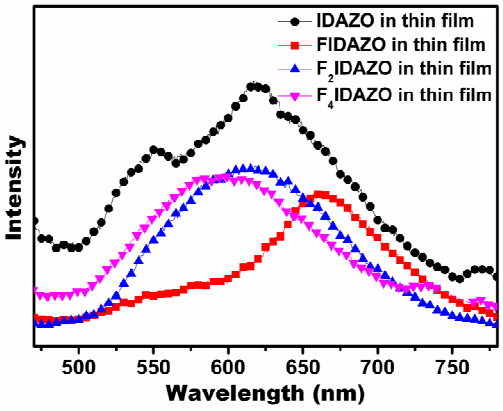

Figure S16. The emission spectra of IDAZO, FIDAZO, F_2IDAZO and F_4IDAZO in thin films on a quartz plate at the same excitation wavelength (λ_{ex} = 460 nm).

Table S1. Optical and electrochemical properties of IDAZO, FIDAZO, F_2IDAZO and F_4IDAZO

compound	absorption λ_{max} (nm) solution[a]	film[b]	λ_{edge} (nm) film[b]	E_g[c] [eV]	E_{ox}(onset)[d] [eV]	HOMO[e] [eV]	LUMO[f] [eV]	Hole[g] [eV]	Electron[h] [eV]
IDAZO	424	433	506	2.45	0.66	–5.12	–2.67	0.32	1.63
FIDAZO	425	393	520	2.38	1.21	–5.67	–3.29	0.87	1.01
F_2IDAZO	427	412	529	2.34	1.34	–5.80	–3.46	1.00	0.84
F_4IDAZO	430	410	532	2.33	1.68	–6.14	–3.81	1.34	0.49

[a] In CH_2Cl_2 solution at 10^{-4} M; [b] Deposited thin films; [c] Estimated from the absorption onset of thin films: $E_g = 1240/\lambda_{edge}$; [d] Vs Ag/AgCl; [e] Determined by the onset of the oxidation peak of CVs; [f] Estimated by subtracting E_g from E_{HOMO}; [g] The difference between the work function of ITO and the HOMO energy level; [h] The difference between the work function of Al and the LUMO energy level.

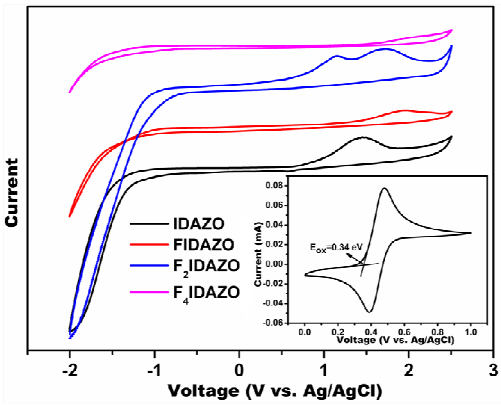

Figure S17. Cyclic voltammograms of IDAZO, FIDAZO, F_2IDAZO and F_4IDAZO with the scan rate of 100 mV s^{-1}.

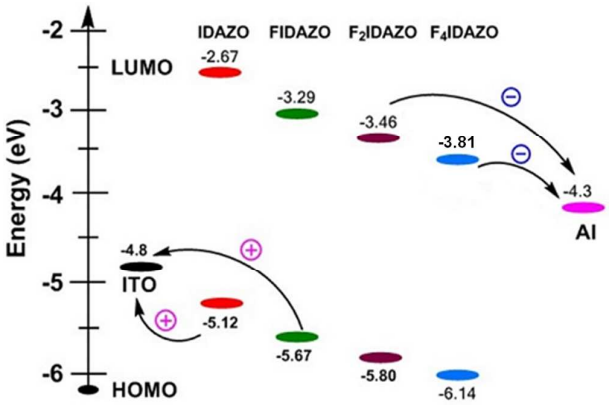

Figure S18. HOMO and LUMO orbital energy levels diagram of IDAZO, FIDAZO, F_2IDAZO and F_4IDAZO along with the work functions of the electrodes (ITO and Al).

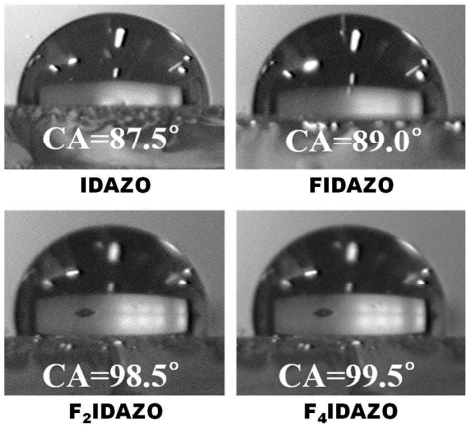

Figure S19. The wettability tests of IDAZO, FIDAZO, F_2IDAZO and F_4IDAZO films under ambient air condition; CA is short for contact angle.

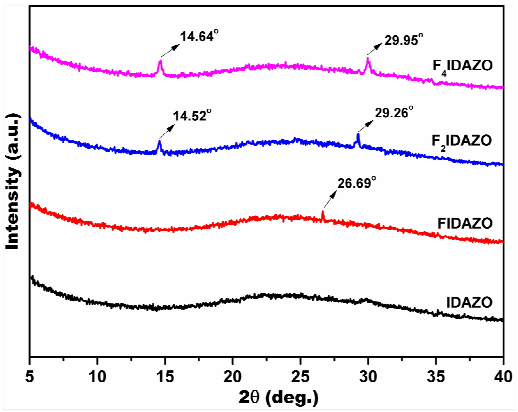

Figure S20. XRD patterns of IDAZO, FIDAZO, F_2IDAZO and F_4IDAZO deposited

films.

References

(1) Miao, S.; Li, H.; Xu, Q.; Li, N.; Zheng, J.; Sun, R.; Lu, J.; Li, C.-M., Molecular Length Adjustment for Organic Azo-Based Nonvolatile Ternary Memory Devices. *J. Mater. Chem.* **2012**, *22*, 16582-16589.

(2) Yu, B.; Shirai, Y.; Tour, J. M., Syntheses of New Functionalized Azobenzenes for Potential Molecular Electronic Devices. *Tetrahedron* **2006**, *62*, 10303-10310.

(3) Zhang, X.; Xu, Y.; Giordano, F.; Schreier, M.; Pellet, N.; Hu, Y.; Yi, C.; Robertson, N.; Hua, J.; Zakeeruddin, S. M.; Tian, H.; Grätzel, M., Molecular Engineering of Potent Sensitizers for Very Efficient Light Harvesting in Thin-Film Solid-State Dye-Sensitized Solar Cells. *J. Am. Chem. Soc.* **2016**, *138*, 10742-10745.

(4) Gu, Q. F.; He, J. H.; Chen, D. Y.; Dong, H. L.; Li, Y. Y.; Li, H.; Xu, Q. F.; Lu, J. M., Multilevel Conductance Switching of a Memory Device Induced by Enhanced Intermolecular Charge Transfer. *Adv. Mater.* **2015**, *27*, 5968-5973.

(5) He, B.; Pun, A. B.; Klivansky, L. M.; McGough, A. M.; Ye, Y.; Zhu, J.; Guo, J.; Teat, S. J.; Liu, Y., Thiophene Fused Azacoronenes: Regioselective Synthesis, Self-Organization, Charge Transport and Its Incorporation in Conjugated Polymers. *Chem. Mater.* **2014**, *26*, 3920-3927.